Mol. Cryst. Liq. Cryst., Vol. 546: pp. 45/[1515]–56/[1526], 2011
Copyright © Taylor & Francis Group, LLC
ISSN: 1542-1406 print/1563-5287 online
DOI: 10.1080/15421406.2011.571607

Taylor & Francis
Taylor & Francis Group

Slow Molecular Processes in a Liquid Crystal Embedded in Aerosil Matrix: Nuclear Magnetic Relaxometric Study

M. RAJESWARI,[1] SURAJIT DHARA,[1] K. VENU,[1]* V. S. S. SASTRY,[1] AND R. DABROWSKI[2]

[1]School of Physics, University of Hyderabad, Hyderabad, India
[2]Institute of Chemistry, Military University of Technology, Warsaw, Poland

Frequency dispersion studies on proton spin-lattice relaxation rates of a liquid crysal (4'-octyloxy-4-cyanobiphenyl) embedded in Aerosil matrix show significant increase at low frequencies (sub-MHz regime) relative to the bulk sample, and are interpreted as primarily due to slow reorientations near the surface ordered layers mediated by translation displacements. The computed exponent in the power law behavior of the dispersion profiles at different temperatures in the isotropic phase indicates an enhanced role of the low-wavelength diffusion modes during this process. The data also show critical contribution near the isotropic-nematic transition to the length scales relevant to adsorption kinetics.

Keywords Liquid crystal; molecular dynamics; nuclear magnetic relaxometry; porous media

1. Introduction

Dynamical behavior of liquid crystals immersed into various porous matrices has been attracting considerable attention over the recent years [1]. Typical examples of such matrices are anopore [2], aerogel [3], controlled porous glass (CPG) [4,5], vycor glass [6], millipore [7,8], nucleopore [9] and Aerosil [10–15]. LC-Aerosil mixtures are particularly interesting because the random disorder can be introduced into the system in a controlled manner by changing the concentration of the silica particles. At very low concentrations (less than 0.01 g/cm^3), the few silica particles added to the LC act as just impurities in the LC medium, as their number is too small to form a 3-d network. In the density range of 0.01 to 0.1 g/cm^3, these particles tend to form a 3-d network due to the inter-particle hydrogen bonds [16] referred as soft

*Present address: Soctronics Technologies Pvt. Ltd., Banjanra Hills, Hyderabad 500 034, India.

Address correspondence to M. Rajeswari, School of Physics, University of Hyderabad, Hyderabad 500 046, India. Tel.: +91-40 23011033; Fax: +91-40 23010227; E-mail: raji.hcu@gmail.com

gel. When the concentration is further increased, the network becomes more rigid and the resulting dispersion becomes a stiff-gel.

Interestingly changes in the physical properties of liquid crystals confined to such Aerosil matrices were studied by various experimental techniques [10–18]. The DNMR [16,17] results in the nematic and smectic phases showed how the field anneals the random disorder introduced by the Aerosil particles upto a certain concentration, beyond which, *i.e.*, in the so called stiff-gel regime, disordering effects completely dominate. Previous proton NMR studies [18] in LC-Aerosil systems showed a clear evidence of an increase in the spin-lattice relaxation rate at very low frequencies (below MHz), and this was explained qualitatively in terms of an extra relaxation mechanism mediated by slow molecular processes near the surface of the porous medium arising from LC-surface interactions.

In the present work, we report our NMR results on 8OCB-Aerosil systems at two concentrations of Aerosil particles (section-2). The appropriate analytical models to account for the observed relaxation rate are discussed in section-3. We analyze the data based on a random walk model which takes into account the LC-surface interaction and the resulting slow time scales as seen by the NMR experiment (section-4). The results are discussed in the light of pretransitional effects near the transition temperature.

2. Experimental Methods

Pure sample of 8OCB was synthesized in our laboratory (Warsaw), and has the phase sequence: I 80°C N 67°C SmA 54.5°C Cr. The liquid crystal-Aerosil mixtures were prepared using solvent method [11]. A hydrophilic Aerosil (type A300), obtained from Degussa Corp., was first dried under vacuum at 200°C overnight, before adding it to the liquid crystal dissolved in pure acetone. After sonicating the mixture for about 2 hours to achieve homogeneous dispersion, the solvent was removed through evaporation at 60°C for a long time, and was sealed in the NMR sample tube under vacuum. Aerosil (A300) consists of small silica spheres of 7 nm in diameter and has a specific surface area of $300\,m^2/g$. The surface of the spheres is covered with hydroxyl groups that interact with each other and form hydrogen bonding between the spheres, leading to a three dimensional network within the liquid crystal environment. The density of silica in our samples is 0.05 and $0.07\,g/cm^3$ (sample-A and sample-B, respectively). The interaction of the hydroxyl groups on the surface of the Aerosil particles with the polar liquid crystal is known to lead to a homeotropic alignment of LC molecules near the surfaces. The shift of the nematic-isotropic transition temperature in both the mixtures is less than 1 K as compared to the bulk sample. The mean void size in these systems is calculated [19] to be 133 nm and 95 nm in samples A and B, respectively.

Proton spin-lattice relaxation times T_1 at different Larmor frequencies ν ($\omega = 2\pi\nu$) were measured covering the range 10 kHz to 50 MHz, on a commercial fast field cycling NMR relaxometer (Stelar Spinmaster FFC 2000) and a homemade pulsed field NMR spectrometer. At higher frequencies (MHz regime) an inversion-recovery pulse sequence was used. On the field-cycling relaxometer (covering the range 10 kHz to 10 MHz), a different sequence ($B_{H\to L}$-τ_i-$B_{L\to H}$-P) leading to a free induction decay was employed. Here τ_i is the evolution time, B_H and B_L are high and low magnetic fields respectively, and P is the radio-frequency pulse causing the magnetization rotation by $\pi/2$ under resonant condition. The time dependence of magnetization recovery was found to be

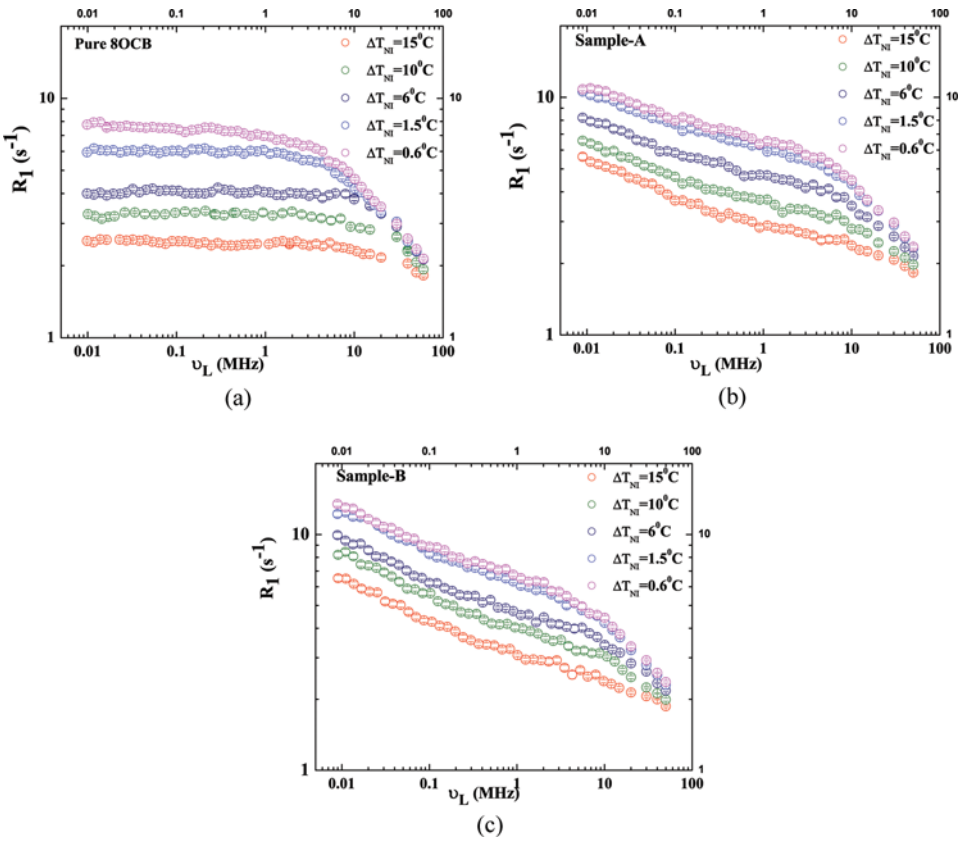

Figure 1. Frequency dispersion of the proton spin-lattice relaxation rate profiles in the isotropic phase at different temperatures (a) Bulk 8OCB, (b) Sample-A, (c) Sample-B.

exponential over the observation time scale. T_1 measurements are accurate to within 3%, while the temperature of the sample was controlled through Stelar unit to within 0.2 K.

Figures 1 and 2 show the frequency and temperature dependences of proton relaxation rate $R_1 = T_1^{-1}$ in the isotropic phase of the bulk and confined 8OCB at the two different concentrations, clearly bringing out the low frequency enhancement of the relaxation rate due to confinement. The temperature dependence of R_1, measured at two frequencies, 0.4 MHz and 12 kHz, shows an enhancement in the relaxation rate even 15 K above T_{NI}.

3. Relaxation Mechanisms in Bulk and Confined Systems

Proton spin-lattice relaxation occurs via the time modulation of dipole-dipole interactions of spin pairs, and in the isotropic phase it is effectively mediated by both inter- and intra-molecular dipolar interactions arising from individual molecular processes [20,21]. These typically occur in the nano second (ns) range, leading to observable dispersion features in the range 10^7–10^8 Hz. Close to T_{NI}, short-range nematic order develops in the isotropic phase, and the life times of this order increases as the clearing point is reach from above. This reflects in the critical

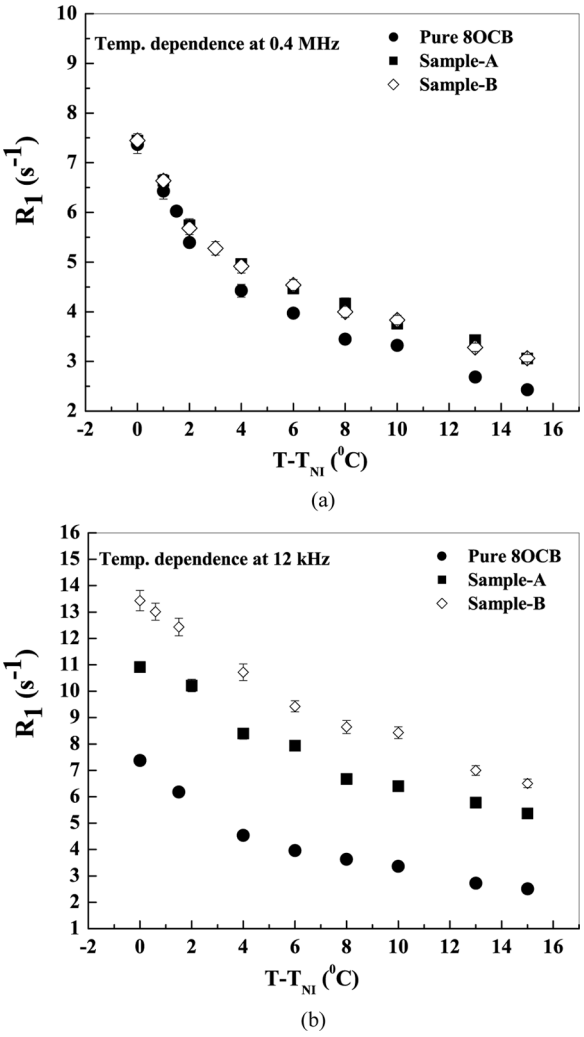

Figure 2. Temperature dependence of proton spin-lattice relaxation rate at two Latmor frequencies for 8OCB in the bulk and Samples A and B.

dependence of the associated correlation times among molecular reorientations. The total spin-lattice relaxation rate R_1 in the bulk isotropic system is thus expressed as [21]

$$R_{1B} = R_{1SD} + R_{1R} + R_{1CF} \tag{1}$$

The first term takes into account the contribution from molecular translational self-diffusion, as it modulates in time the dipole-dipole interaction among spins, particularly via inter-molecular spin interactions. Its contribution in viscous isotropic liquids was computed earlier [22], needing two fitting parameters: the coupling constant B and the diffusion coefficient D. This can be expressed as

$$R_{1SD} = \frac{B}{\omega}[f(\alpha, x) + f(\alpha, \sqrt{2}x)].$$

Where

$$\alpha = \frac{\langle r^2 \rangle}{12a^2}, \quad x = \left(\frac{\omega a^2}{D}\right)$$

$$f(\alpha, x) = \frac{2}{x^2}\left\{ v\left[1 - \frac{1}{(u^2+v^2)}\right] + \left[v\left(1 + \frac{1}{(u^2+v^2)}\right) + 2\right] e^{-2v} cos2u \right.$$
$$\left. + u\left[1 - \frac{1}{(u^2+v^2)}\right] e^{-2v} sin2u \right\}$$
$$\begin{pmatrix} u \\ v \end{pmatrix} = \frac{(\omega a^2/2D)^{1/2}}{(4+\omega^2\tau^2)^{1/4}} \left\{ 1 \pm \frac{\omega\tau}{(4+\omega^2\tau^2)^{1/2}} \right\}^{1/2}.$$

The second term represents the contribution from molecular reorientations characterized by the correlation time $\tau_{R,}$ and is given by [23]

$$R_{1R} = A_R \sum_{p=1}^{2} \frac{p^2 \tau_R}{1 + (p\omega\tau_R)^2}.$$

Here A_R is the coupling constant quantifying the contribution from reorientations. In the limit of fast reorientations, $\omega\tau_R << 1$, the above contribution becomes essentially frequency independent and is constant over the frequency region of our experiment at a given temperature.

The third term comes from the time-modulation of dipolar interactions due to short-range nematic order fluctuations. This contribution is expressed as [21,24]:

$$R_{1CF} = A_{CF} \left[\frac{\tau_{CF}}{1 + \sqrt{1 + \omega^2 \tau_{CF}^2}} \right]^{1/2}.$$

Here $A_{CF} = AT\sqrt{\eta}$ is a temperature dependent parameter, providing a measure of the contribution of short-range nematic order fluctuations. τ_{CF} is the average correlation time of the short-range nematic order fluctuations and η is the effective viscosity. The correlation time τ_{CF} is further written in terms of the correlation length ξ as

$$\tau_{CF} = \frac{\eta \xi^2}{L}$$

Where

$$\xi = \sqrt{\frac{L}{a(T - T_{NI}^*)^{\gamma}}}$$

L is related to the elastic constants, a is the temperature independent coefficient in the Landau expansion of the relevant free energy, and γ is the associated exponent (which is unity in the mean field approximation).

The confinement of liquid crystals introduces a new relaxation mechanism contributing to the total relaxation rate. The interaction of the liquid crystal molecules with the surfaces induces local order relative to the surface. In this context, it is convenient to view a confined LC system to consist of two phases: a bulk like phase away from the surface where the orientational order parameter is zero, and a surface ordered phase close to the surfaces where fast molecular reorientations are spatially restricted and the orientational order parameter takes a finite value. The surface ordered phase has a finite thickness determined by the relative strengths of the two ordering mechanisms. Thus a confining nanoporous system presents a more complex scenario of molecular processes, with liquid crystal molecules exchanging between these two dynamically different organizations. A simplification is usually made by assuming that a fast molecular exchange takes place between the two phases. The reorientations of the molecules occurring due to translational diffusion near the ordering surface (RMTD) have a different time scale, and slower relative to bulk medium, because of the surface induced preferred orientation and relatively smooth (at molecular level) surface of the pores (providing topologically a two dimensional surface). This mechanism has been explored in detail earlier [25,26].

Within the two-phase fast exchange regime, the RMTD process describes molecular reorientations caused by the diffusional displacement of LC molecules on the surface of the pore. The time correlation function for the RMTD process consequently contains dynamic as well as geometrical information on the system. The dynamical part refers to the translational diffusion and the geometrical part refers to the surface topology of the pores in the matrix. The general correlation function for RMTD is given by

$$G(t) = \int_0^\infty S(k) e^{-Dtk^2} dk$$

Where $S(k)$ is the orientational structure factor: k refers to the wave vector. The corresponding spectral density is given by

$$J(\omega) = \int_0^\infty G(t)\cos(\omega t)dt = \int_0^\infty S(k)\frac{2\tau_k}{1+\omega^2\tau_k^2}dk$$

Where

$$\tau_k = \frac{1}{Dk^2}.$$

The relaxation rate $R_{1RMTD} = (T_1^{-1})_{RMTD}$ in confined liquid crystals above T_{NI} can be expressed as [27,30]

$$(R_1)_{RMTD} = \frac{A_{RMTD}}{\omega^p}\left[f\left(\frac{\omega_{RMTD\max}}{\omega}\right) - f\left(\frac{\omega_{RMTD\min}}{\omega}\right)\right] + \frac{4A_{RMTD}}{2^{1/2}\omega^p}\left[f\left(\frac{\omega_{RMTD\max}}{2\omega}\right) - f\left(\frac{\omega_{RMTD\min}}{2\omega}\right)\right]$$

where

$$f(y) = \frac{1}{\pi}\left[arctan\left(\sqrt{2y}+1\right) + arctan\left(\sqrt{2y}-1\right) - arctan\,h\left(\frac{\sqrt{2y}}{y+1}\right)\right]$$

Here $\omega_{RMTDmin} = Dk^2_{min}$ and $\omega_{RMTDmax} = Dk^2_{max}$ are the minimum and maximum cutoff frequencies, which are in turn related to the corresponding length scales $L_{max} = (\omega_{RMTDmin})^{-1}$ and $L_{min} = (\omega_{RMTDmax})^{-1}$. The relaxation rate in the confined systems now includes additional RMTD mechanism, and hence the observed relaxation rate is expressed as

$$R_{1C} = R_{1SD} + R_{1R} + R_{1CF} + R_{IRMTD} \tag{2}$$

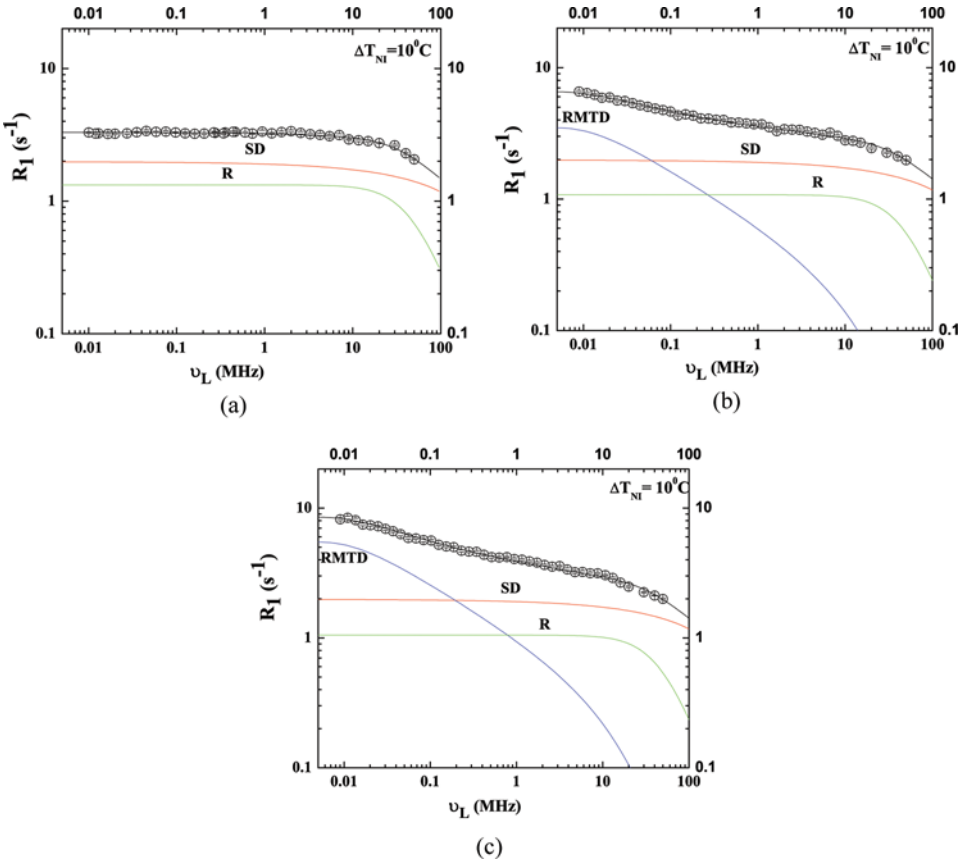

Figure 3. Frequency dependence of proton spin-lattice relaxation rate of 8OCB at $\Delta T_{NI} = 10^{\circ}C$ (a) Bulk 8OCB, (b) Sample-A, (c) Sample-B. The black line is the calculated total relaxation rate obtained by using Eqs. 1 & 2. Color lines are the corresponding relaxation rate contributions from different mechanisms as shown in the figures.

4. Results and Discussion

The dispersion data at different temperatures were fit to Eq. (1) in the case of bulk sample and Eq. (2) for confined system. Non-linear least squares method was used to get the best fit parameters consistent with frequency and temperature dependences. Diffusion data were available from other experiments [28,29] and so D was not a variable in the analysis. We find that the coupling constant B is fairly insensitive to temperature and so we took the average value and used the same at all temperatures. The prefactor A_R and the reorientational correlation time τ_R show temperature dependences as expected in liquid crystals. As we approach the nematic-isotropic transition, the contribution from critical fluctuation becomes significant, and is reflected in the plots showing relative contributions of different mechanisms (Figure 4). We find that the τ_{CF} values (obtained from bulk sample data) are comparable to those in other LC systems, like 6CHBT [31]. The fitted curves and parameters are shown in Figures 3 and 4 and Table 1.

While analyzing the dispersion profiles of the confined system using Eq. (2), we take advantage of the knowledge of the dynamic behavior in the bulk sample and

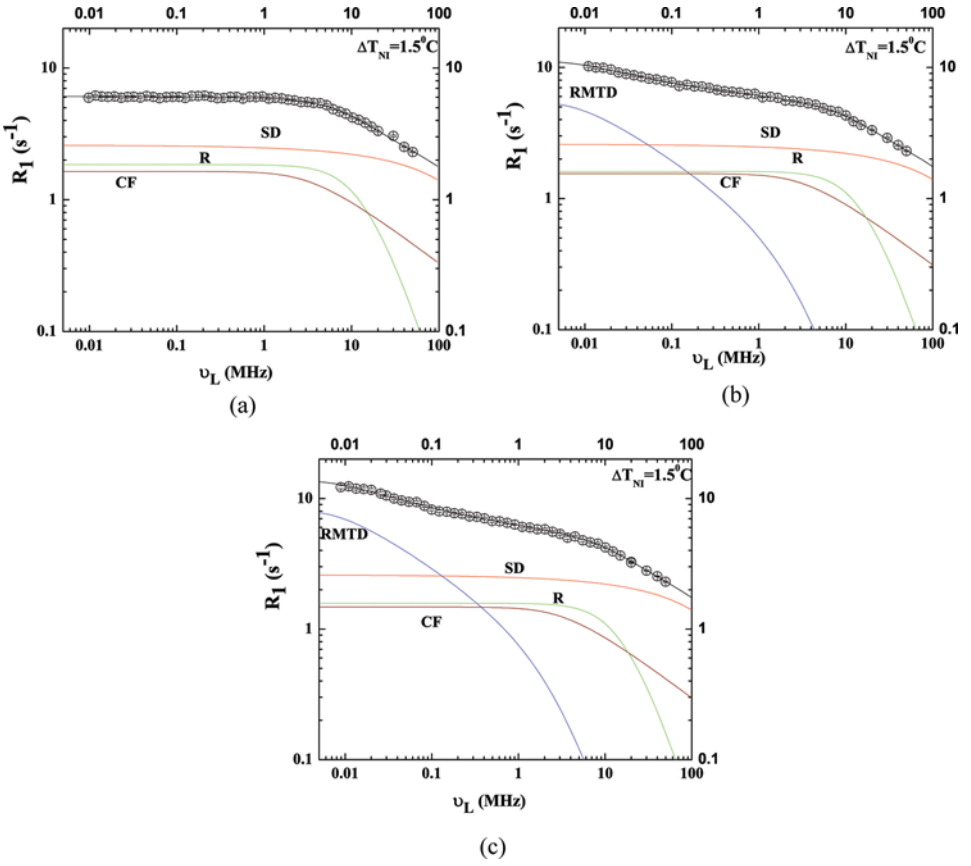

Figure 4. Frequency dependence of proton spin-lattice relaxation rate of 8OCB at $\Delta T_{NI} = 1.5°C$ (a) Bulk 8OCB, (b) Sample-A, (c) Sample-B. The black line is the calculated total relaxation rate obtained by using Eqs. 1 & 2. Color lines are the corresponding relaxation rate contributions from different mechanisms as shown in the figures.

Table 1. Best fit parameters for the bulk and confined 8OCB systems

Parameter	Bulk 8OCB					Sample-A					Sample-B				
ΔT_{NI} (°C)	15	10	6	1.5	0.6	15	10	6	1.5	0.6	15	10	6	1.5	0.6
B (10^{10}) s^{-2}			0.25					0.25					0.25		
D (10^{-10}) m^2/s	1.91	1.61	1.41	1.23	1.19	1.91	1.61	1.41	1.23	1.19	1.91	1.61	1.41	1.23	1.19
A_R (10^9) s^{-2}	0.95	0.75	0.33	0.27	0.25	0.95	0.75	0.33	0.27	0.25	0.95	0.75	0.33	0.27	0.25
τ_R (10^{-9}) s	0.91	1.77	2.81	6.86	7.86	0.78	1.77	2.81	5.97	6.72	0.78	1.77	2.75	5.84	6.55
A_{CF} (10^3) $s^{-3/2}$	–	–	7	8.3	9.6	–	–	6.13	7.89	8.59	–	–	5.19	7.52	8.4
τ_{CF} (10^{-9}) s	–	–	35	77	183	–	–	35	77	183	–	–	35	77	183
p			–					0.38					0.38		
A_{RMTD} (10^2 $s^{-(1+p)}$)			–			0.6	0.67	0.82	0.9	0.95	0.81	1.07	1.1	1.35	1.5
$\omega_{RMTDmin}/2\pi$ (10^3 Hz)			–			15	14	12	9	8	15	14	12	9	8
$\omega_{RMTDmax}/2\pi$ (10^7) Hz			–			6.5	4.5	2.8	0.6	0.1	6.5	4.5	2.8	0.6	0.1

hence focus primarily on the RMTD mechanism. Thus the fit parameters in this case pertain to the lower and upper cutoff frequencies ($\omega_{RMTDmin}$ and $\omega_{RMTDmax}$) and the exponent p in the assumed power law behavior for the frequency dispersion between these two frequency limits [27]. We find that the data in this region fit to $(T_1^{-1})_{RMTD} \propto \omega^{-p}$, with $p = 0.38 \pm 0.04$. Deviation of p from the equipartition value of 0.5 [27,30] point out to the relatively higher weight accorded to lower wavelength modes of diffusion in this confined system, arising from the surface topology. The cutoff frequencies $\omega_{RMTDmin}$ and $\omega_{RMTDmax}$ are related to the largest and smallest molecular displacements, needed to cause appreciable loss of correlation among the orientation of molecules, L_{max} and L_{min}, respectively [30]. The estimated value of $L_{max} = 91 \pm 6$ nm does not show significant variation with the temperature, while that of L_{min} shows a substantial change with temperature, particularly near the transition temperature indicating the role of pretransitional effects on the surface diffusion characteristics of the molecules. This points to enhanced ordering near the surface over extended regions as the system approaches the transition region. This pretransitional effect on L_{min} is shown in Figure 5.

The strength of the RMTD interaction A_{RMTD} shows an Arrhenius behavior with temperature at both the concentrations (sample-A and sample-B) as shown in Figure 6, and it is enhanced in sample-B, relative to sample-A, due to its dependence on the diffusion coefficient, surface order parameter and the fraction of molecules in the surface layer. The corresponding activation energies at the two concentrations are: $E_a = 35$ kJ/mole for sample-A and 41.5 kJ/mole for sample-B. The slight increase in the activation energy at higher concentration might be due to an increased attractive interaction between Aerosil matrix and the liquid crystal molecules at the surface. We did not find observable variation in the two cutoff frequencies for the two samples. It may also be noted that the values of τ_R (related to molecular reorientation mechanism) in the two samples differ slightly, especially near the transition temperature, indicating corresponding changes in the

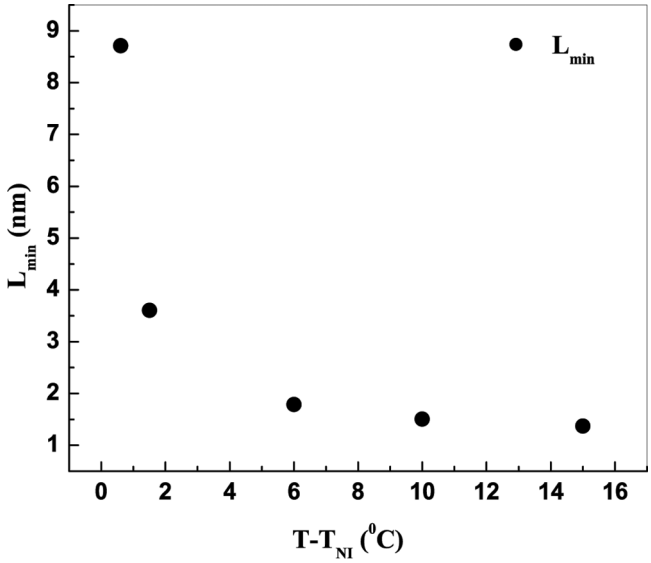

Figure 5. Temperature variation of L_{min} (see the text).

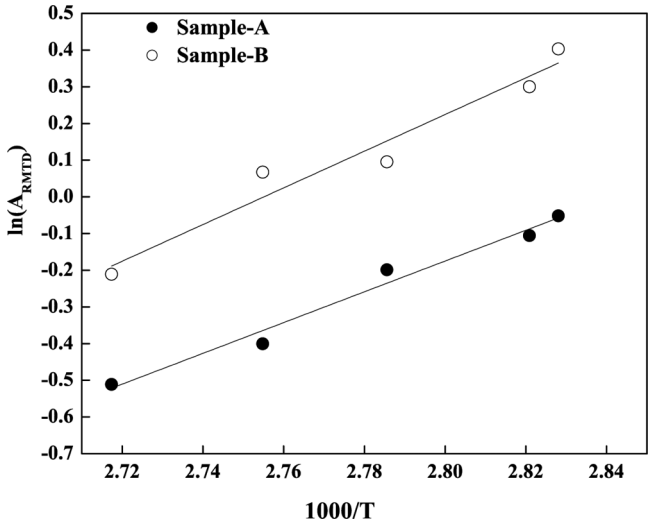

Figure 6. Temperature variation of A_{RMTD} at different Aerosil concentrations. The solid line shows the best Arrhenius fit of the experimental data.

orientational ordering in the system. In comparison, there have been only very marginal changes in A_R in the confined samples relative to its values in the corresponding bulk systems, and keeping the errors of analysis in view its bulk values are used in computing the contributions from this mechanism (Table 1).

5. Conclusions

In this paper we report proton spin-lattice relaxation rate measurements in the isotropic phase of bulk 8OCB and 8OCB confined to Aerosil matrix at two different concentrations. We found a notable increase in the relaxation rates in the sub-MHz regime. This observed significant increase is quantitatively explained in terms of an additional slow relaxation mechanism of molecular reorientations mediated by translational displacements (RMTD), and it is characterized by power-law dispersion in the frequency range between low and high frequency cutoff values. The analysis of the experimental data shows that the major increase in the relaxation rate is due to this process. The low and high frequency cutoffs of the RMTD mechanism provide some insight into how the molecules are reorienting at the surface. The exponent value indicates that the relative importance of low wavelength modes has increased compared to expectation from equipartition distribution, and it is different from the other confined systems studied in the isotropic phase [27,30]. The increased interaction strength of this mechanism on increasing the concentration of Aerosil particles shows that the fraction of molecules in the ordered layer has correspondingly increased.

Acknowledgment

MR would like to thank the University Grants Commission, New Delhi for providing RFSMS fellowship.

References

[1] Liquid crystals in complex geometries. (1996). In: Crawford, G. P., & Zumer, S. (Eds.), Taylor & Francis: London.
[2] Germano, S. Iannacchione & Daniel Finotello. (1992). *Phys. Rev. Lett.*, *69*, 2094.
[3] Clark, Noel A., Bellini, Tommaso, Malzbender, Rainer M., Thomas, Britt N., Rappaport, Aqron G., Muzny, Chris D., Schaefer, Dale W., & Hrubesh, Larry (1993). *Phys. Rev. Lett.*, *71*, 3505.
[4] Kralj, S., Zidansek, A., Lahajnar, G., Musevic, I., Zumer, S., Blinc, R., & Pintar, M. M. (1996). *Phys. Rev. E*, *53*, 3629.
[5] Dadmun, M. D., Muthukumar, M. (1993). *J. Chem. Phys.*, *98*, 4850.
[6] Iannacchione, G. S., Crawford, G. P., Zumer, S., Doane, J. W., & Finotello, D. (1993). *Phys. Rev. Lett.*, *71*, 2595.
[7] Sihai Qian, Germano, Iannacchione, S., & Daniele Finotello. (1998). *Phys. Rev. E*, *57*, 4305.
[8] Finotello, D., Zeng, H., Zalar, B., & Iannacchione, G. S. (2001). *Mol. Cryst. Liq. Cryst.*, *358*, 237.
[9] Allender, D. W., Crawford, G. P., & Doane, J. W. (1991). *Phys. Rev. Lett.*, *67*, 1442.
[10] Zhou, B., Iannacchione, G. S., Garland, C. W., & Bellini, T. (1997). *Phys. Rev. E*, *55*, 2962.
[11] Iannacchione, G. S., Garland, C. W., Mang, J. T., & Rieker, T. P. (1998). *Phys. Rev. E*, *58*, 5966.
[12] Bellini, T., Radzihovsky, L., Toner, J., & Clark, N. A. (2001). *Science*, *294*, 1074.
[13] Bellini, T., Buscaglia, M., Chiccoli, C., Mantegazza, F., Pasini, P., & Zannoni, C. (2002). *Phys. Rev. Lett.*, *88*, 245506.
[14] Clegg, P. S., Stock, C., Birgeneau, R. J., Garland, C. W., Roshi, A., & Iannacchione, G. S. (2003). *Phys. Rev. E*, *67*, 021703.
[15] Roshi, A., Iannacchione, G. S., Clegg, P. S., & Birgeneau, R. J. (2004). *Phys. Rev. E*, *69*, 031703.
[16] Jin, T., & Finotello, D. (2001). *Phys. Rev. Lett.*, *86*, 818.
[17] Jin, T., & Finotello, D. (2004). *Phys. Rev. E*, *69*, 041704.
[18] Anoardo, E., Grinberg, F., Vilfan, M., & Kimmich, R. (2004). *Chem. Phys.*, *297*, 99.
[19] Iannacchione, Germano S. (2004). *Fluid Phase Equilibria*, *222–223*, 177.
[20] Abragam, A. (1961). *The Principles of Nuclear Magnetism*, Clarendon Press: Oxford.
[21] Dong, R. Y. (1994). *Nuclear Magnetic Resonance of Liquid Crystals*, Springer-Verlag.
[22] Torrey, H. C. (1953). *Phys. Rev.*, *92*, 962.
[23] Bloembergen, N., Purcell, E. M., & Pound, R. V. (1948). *Phys. Rev.*, *73*, 679.
[24] Chavez, F. V., Bonetto, F., & Pusiol, D. J. (2000). *Chem. Phys. Lett.*, *330*, 368.
[25] Kimmich, R., & Weber, Hans Werner. (1993). *Phys. Rev. B*, *47*, 11788.
[26] Kimmich, R., & Anoardo, E. (2004). *Prog. Nucl. Magn. Reson. Spectrosc.*, *44*, 257.
[27] Sebastiao, P. J., Sousa, D., Ribeiro, A. C., Vilfan, M., Lahajnar, G., Seliger, J., & Zumer, S. (2005). *Phys. Rev. E*, *72*, 061702.
[28] Mager, J. O. (1993). *Ph.D. Thesis*, University of Stuttgart.
[29] Cifelli, M., McDonald, P. J., & Veracini, C. A. (2004). *Phys. Chem. Chem. Phys*, *6*, 4701.
[30] Vilfan, M., Apih, T., Sebastiao, P. J., Lahajnar, G., & Zumer, S. (2007). *Phys. Rev. E*, *76*, 051708.
[31] Phanikumar, B. V. N., Satheesh, V., Venu, K., Sastry, V. S. S., & Dabrowski, R. (2009). *Phase Transitions.*, *82*, 131.